

# Design of stand alone PV system for DC-micro grid

Ganesh Baliram Ingale, Subhransu Padhee, Umesh C. Pati

Department of Electronics and Communication Engineering

National Institute of Technology

Rourkela, Odisha, India

ganasha4191@gmail.com, subhransupadhee@gmail.com, ucpati@nitrkl.ac.in

**Abstract**—This paper provides modeling of photovoltaic (PV) panel, designing of maximum power point tracking (MPPT) control algorithm for a standalone PV based distributed generation (DG) system. A detailed mathematical model of PV panel is provided. One of the most classical MPPT (Perturb and Observe MPPT) is used to track the maximum power point of the system. SunPower PV array are considered and simulation results showcase the module characteristics and array characteristics. A detailed design technique is provided for MPPT technique and simulation are carried out with varying solar irradiance.

**Keywords**—Photovoltaic; MPPT; Distributed Generation (DG); micro-grid

## I. INTRODUCTION

DC micro grid is an energy network which comprises of renewable energy sources (RES) and storage devices. The main benefit of the micro grid system is that it can be locally controlled and the energy can be provided to local grid or can be consumed in a stand-alone manner [1]. Micro grids are very much useful during natural disasters and it improves the performance and overall efficiency of the transmission as well as distribution network. Substantial amount of research has been carried out in the functionality and control aspect of DC micro grid. DC micro grid with PV panels and battery (ultra-capacitor and Li-ion batteries) can easily mitigate and solve some real operational issues [2].

Due to ever increasing demand for energy, scientists are working towards RES such as Photovoltaic (PV), fuel cell and wind energy. Out of the different renewable energy sources PV is used widely across the globe because of its relatively moderate cost and abundant availability of solar power. PV generation plant can be used either in standalone mode or in grid connection mode. The output voltage of PV panel varies with varying solar irradiation and ambient temperature. The maximum power point tracking (MPPT) mechanism provides the maximum power at any environmental condition. MPPT is integrated with power electronic converter which eventually provides a regulated power to the load. The basic components of a PV based system are PV panel, MPPT controller and a power conditioning unit (PCU). The PCU consists of one or more than one power electronic converter depending upon the specific application. The most widely used PCU configuration is two stage PCU configurations comprising of a DC-DC converter and DC-AC inverter. The converter regulates the

voltage of PV cell and the inverter inverts the voltage to utility AC signal which can then be integrated to the utility grid. The demand of the day is to make PV affordable for masses and compact in size and weight perspective. Microcontroller based real time implementation of PV based system is reported in [3], [4].

The efficiency of the commercial PV panels is relatively low, so a significant power gets wasted. The major challenge is to tackle the nonlinear output characteristics of a PV panel with unpredictable changes in solar irradiance and ambient temperature. To maximize the power output of the panel, MPP has to be tracked efficiently. This paper provides a comprehensive analysis of different aspects of modeling of PV cell, designing a MPPT control algorithm and providing power to a DC-micro grid. Complete mathematical model of PV cell has been carried out and the effect of solar irradiance and change of ambient temperature has been investigated. Classical perturb and observe MPPT algorithm has been utilized to extract maximum power from the panel.

The rest of the paper is organized as follows. Section II provides a detailed mathematical model of PV cell. Section III discusses about perturb and observe MPPT algorithm. Section IV provides an introduction about the power conditioning unit and boost converter. Section V provides simulation results and section VI concludes the paper.

## II. MATHEMATICAL MODEL OF PV CELL

The circuit diagram of a PV cell is illustrated in Fig. 1. The ideal PV cell consists of a constant current source and a diode whereas the practical PV cell consists of additional series  $R_s$  and parallel resistance  $R_p$ . Modeling of PV cell is summarized in [5]–[7].

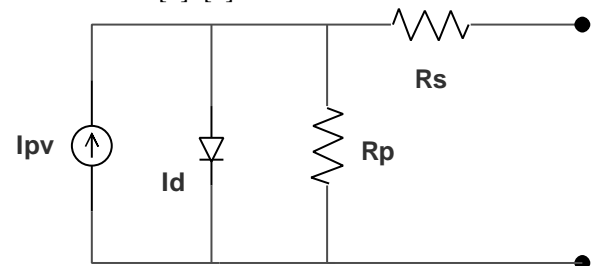


Fig. 1. Circuit diagram of PV cell

The basic equation which describes the I-V characteristics of an ideal PV cell can be represented as

$$I = I_{pv} - I_d \quad (1)$$

Where  $I_{pv}$  is current of PV cell and  $I_d$  is Shockley diode equation which can be represented as

$$I_d = I_o \left[ \exp\left(\frac{qV}{akT}\right) - 1 \right] \quad (2)$$

Therefore, I-V characteristics of an ideal PV cell can be represented as

$$I = I_{pv} - I_o \left[ \exp\left(\frac{qV}{akT}\right) - 1 \right] \quad (3)$$

Where  $I_o$  is the leakage current of diode,  $q$  is electron charge,  $K$  is Boltzmann constant and  $T$  is temperature of p-n junction (Kelvin)

In practice, the series and parallel equivalent characteristics of PV cell can be represented as

$$I = I_{pv} - I_o \left[ \exp\left(\frac{qV}{akT}\right) - 1 \right] - \frac{V + R_s I}{R_p} \quad (4)$$

Where  $R_s$  is series resistance and  $R_p$  is parallel resistance

$V_t$  is thermal resistance of PV cell and  $N_s$  is number of cells connected in series. The thermal resistance of PV cell can be

$$\text{represented as } V_t = \frac{N_s k T}{q}$$

The current of the PV cell is dependent on solar irradiance and temperature. The relation between the PV current and temperature can be represented as

$$I_{pv} = \left( I_{pv,n} + K_I \Delta_T \right) \frac{G}{G_n} \quad (5)$$

where  $I_{pv,n}$  is light generated current at nominal operating condition ( $25^\circ\text{C}, 1000\text{W}/\text{m}^2$ ),  $\Delta_T$  is the difference of temperature (Actual and nominal temperature),  $G$  is the irradiance of the surface and  $G_n$  is the nominal irradiance. The relationship of diode saturation current with temperature can be represented as

$$I_o = I_{o,n} \left( \frac{T_n}{T} \right)^3 \exp \left[ \frac{qE_g}{ak} \left( \frac{1}{T_n} - \frac{1}{T} \right) \right] \quad (6)$$

The nominal saturation current can be expressed as

$$I_{o,n} = \frac{I_{sc,n}}{\exp\left(\frac{V_{oc,n}}{aV_{t,n}}\right) - 1} \quad (7)$$

The modified nominal saturation current can be represented as

$$I_{o,n} = \frac{I_{sc,n} + K_V \Delta_T}{\exp\left(\frac{V_{oc,n} + K_I \Delta_T}{aV_t}\right) - 1} \quad (8)$$

### A. Types of PV Cell

There are different types of PV cells such as mono-crystalline, polycrystalline and thin film. The energy conversion efficiency of mono-crystalline type PV cell is 12 to 15%. Shell SQ85 and PM 648 solar panel are made up of mono-crystalline PV cell. The energy efficiency of polycrystalline and thin film PV cell are 11 to 14% and 6 to 12% respectively. SSI-M6-205 and Shell ST40 PV panels are made up of polycrystalline and thin film PV cells.

TABLE I. PARAMETERS OF MANUFACTURER'S DATASHEET OF DIFFERENT PV CELL

Parameters	Shell SQ85	PM648	SSI-M6-205	Shell ST-40
$I_{sc}$ (A)	5.45	2.8	7.91	2.68
$V_{oc}$ (V)	22.2	21.6	35.55	23.3
$I_{mpp}$ (A)	4.95	2.2	7.31	2.41
$V_{mpp}$ (V)	17.2	18.2	28.04	16.6

### III. MAXIMUM POWER POINT TRACKING

Maximum power point tracking (MPPT) is one of the most vital components of PV system. A large number of MPPT techniques have been reported in literature. The comparative analysis and overview of different MPPT techniques have been reported in [8]–[14]. Fig. 2 shows the block diagram of PV panel with MPPT based control mechanism.

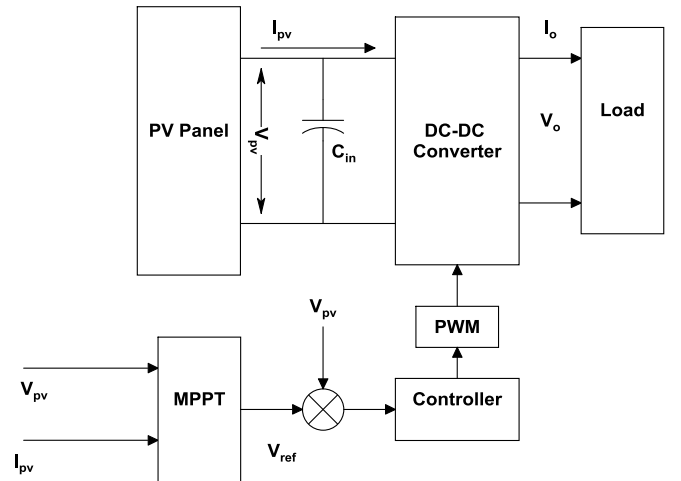


Fig. 2. Block diagram of PV panel with MPPT based control mechanism

One of the most widely used MPPT is Perturb and Observe (P&O) MPPT because it is true MPPT, independent of PV panel, can be implemented using both analog and digital circuit and the technique doesn't require periodic tuning. The

main principle of (P&O) MPPT is the checking of  $\frac{dP}{dV}$  slope.

The slope is positive at the left of MPP and the slope is negative at the right of MPP [15]. This can be mathematically expressed as

$$\frac{dP}{dV} = \begin{cases} > 0 & V < V_{mpp} \\ = 0 & V = V_{mpp} \\ < 0 & V > V_{mpp} \end{cases} \quad (9)$$

Fig. 3 illustrates the algorithm of (P&O) MPPT. Initially the voltage and current of PV module is measured using respective voltage and current sensors and the power is calculated. Change of power and change of voltage is calculated and if the change of power  $dP > 0$  and also  $dV > 0$  then the duty cycle increases by a fraction of  $\Delta D$  and for negative slope the duty cycle decreases by a fraction of  $\Delta D$ . The efficiency of MPPT technique can be calculated using the following formula

$$\eta_{mppt} = \frac{P_{pv}}{P_{mppt}} \times 100 \quad (10)$$

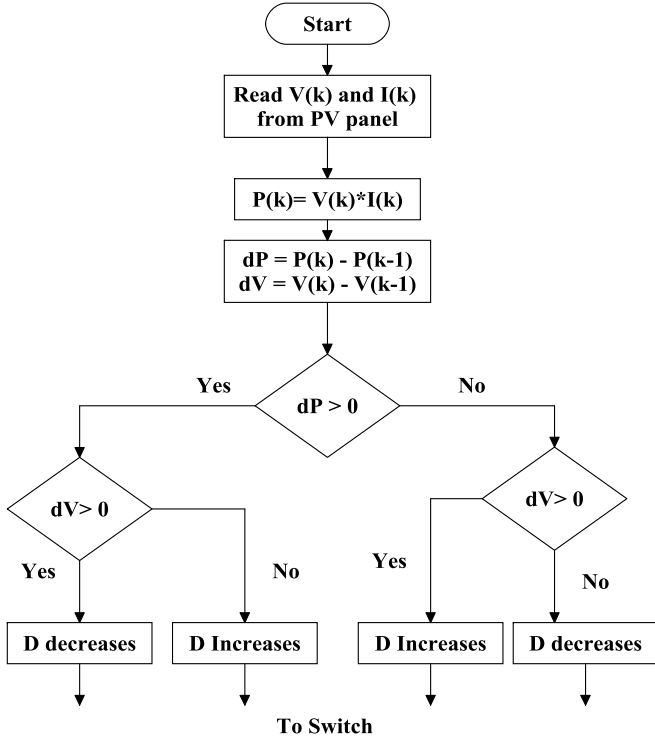


Fig. 3. Flow chart of conventional P&O MPPT algorithm

#### IV. POWER CONDITIONING UNIT

Renewable energy sources provide low voltage output. To use the renewable energy source for utility grid application, the low voltage output needs to be stepped up and inverted. For this purpose, power conditioning unit (PCU) is required.

There are different kinds of PCU topologies available in the literature. The most widely used PCU topology is the multi staged PCU topology. In multi staged PCU topology, a DC-DC converter and a DC-AC inverter is used for the power processing purpose. For grid connectivity, passive LCL filters and transformers are necessary.

##### A. Boost Converter

The boost converter is a DC to DC power converter which can provide an output voltage which is greater than its input voltage. Boost converter is a class of switched mode power converter which contains at least two semiconductor devices i.e a diode and a MOSFET/transistor along with two energy storage element, a capacitor and an inductor. Its input has a inductor which reduces the input current ripple and filter capacitor is normally placed at the output of the boost converter to reduce output voltage ripple. The circuit diagram of classical boost converter is shown in Fig. 4.

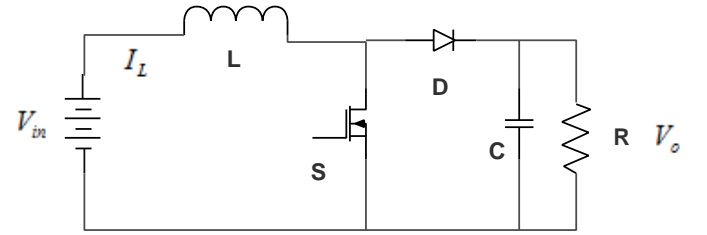


Fig. 4. Circuit diagram of boost converter

The duty ratio of boost converter can be represented as

$$V_o = \frac{V_{in}}{1-D} \quad (11)$$

The inductor  $L$  and capacitor  $C$  values of boost converter can be derived using the maximum allowable inductor ripple current  $\Delta i_L$ , maximum allowable ripple voltage  $\Delta v_c$  and  $f$  is the switching frequency of boost converter. The inductor value can be calculated as

$$L = \frac{V_{in} D}{f \Delta i_L} \quad (12)$$

The capacitor value can be calculated as

$$C = \frac{I_o D}{f \Delta v_c} \quad (13)$$

Switched mode power converter is a time variant nonlinear system where the dynamics is dependent on the state of the switch (whether ON or OFF). Therefore, for each individual state of the switch a different dynamics is obtained. To find the complete model, averaging technique is used. This method is called state space averaging technique which is widely used in power electronics for modeling switched mode power converter. The state space model of the converter at ON state and at OFF state can be represented as

$$\begin{cases} \dot{x} = A_1x + B_1u & t \in [0, dT_s] \\ \dot{x} = A_2x + B_2u & t \in [dT_s, T_s] \end{cases} \quad (14)$$

The inductor current and capacitor voltage are considered as the state variables for the boost converter. During ON state, the state space model of boost converter can be represented as

$$\frac{d}{dt} \begin{bmatrix} i_L \\ v_c \end{bmatrix} = \begin{bmatrix} 0 & 0 \\ 0 & -\frac{1}{RC} \end{bmatrix} \begin{bmatrix} i_L \\ v_c \end{bmatrix} + \begin{bmatrix} \frac{1}{L} \\ 0 \end{bmatrix} V_{in} \quad (15)$$

$$V_o = [0 \quad 1] \begin{bmatrix} i_L \\ v_c \end{bmatrix} \quad (16)$$

During OFF state the state space model of boost converter can be represented as

$$\frac{d}{dt} \begin{bmatrix} i_L \\ v_c \end{bmatrix} = \begin{bmatrix} 0 & -\frac{1}{L} \\ \frac{1}{C} & -\frac{1}{RC} \end{bmatrix} \begin{bmatrix} i_L \\ v_c \end{bmatrix} + \begin{bmatrix} \frac{1}{L} \\ 0 \end{bmatrix} V_{in} \quad (17)$$

$$V_o = [0 \quad 1] \begin{bmatrix} i_L \\ v_c \end{bmatrix} \quad (18)$$

The state space average model can be formulated by combining the two states (ON and OFF) of the converter. The state space average model can be represented as

$$\dot{x} = (A_1d + (1-d)A_2)x + (B_1d + (1-d)B_2)u \quad (19)$$

$$\frac{d}{dt} \begin{bmatrix} i_L \\ v_c \end{bmatrix} = \begin{bmatrix} 0 & -\frac{(1-d)}{L} \\ \frac{(1-d)}{C} & -\frac{1}{RC} \end{bmatrix} \begin{bmatrix} i_L \\ v_c \end{bmatrix} + \begin{bmatrix} \frac{1}{L} \\ 0 \end{bmatrix} V_{in} \quad (20)$$

The generalized small signal transfer function of an ideal boost converter can be represented as

$$\frac{\hat{V}_o(s)}{\hat{d}(s)} = G_{d_0} \left( \frac{\left(1 - \frac{s}{\omega_{z_1}}\right) \left(1 + \frac{s}{\omega_{z_2}}\right)}{\frac{s^2}{\omega_o^2} + \frac{s}{Q\omega_o} + 1} \right) \quad (21)$$

Here

$$G_{d_0} = \frac{V_o}{1-d}, \quad \omega_{z_1} = \frac{R(1-D)^2}{L}, \quad \omega_{z_2} = \infty, \quad \omega_o = \frac{1-D}{\sqrt{LC}},$$

$$Q = R(1-D)\sqrt{\frac{C}{L}}$$

## V. SIMULATION RESULTS

For simulation purpose, Sun Power SPR 305 WHT modules are considered. The parameters of the panel are summarized in Table II. The number of series connected modules or strings are 5. The number of parallel strings is 66. The I-V and P-V characteristics of the PV module are illustrated in Fig. 5. The I-V and P-V characteristics are highly nonlinear and the MPPT algorithm finds the maximum power point. Fig. 6 illustrates the I-V and P-V characteristics of PV array with varying solar irradiance.

TABLE II. SPECIFICATIONS OF SPR 305 WHT PV PANEL

Parameters	Values
Type	Mono crystalline silicon
Power rating at STC	305W
Power per unit area STC	187 W/m <sup>2</sup>
Peak efficiency	18.7%
$V_{mp}$	54.7 V
$I_{mp}$	5.58 A
$I_{sc}$	5.96 A
$V_{oc}$	64.2 V

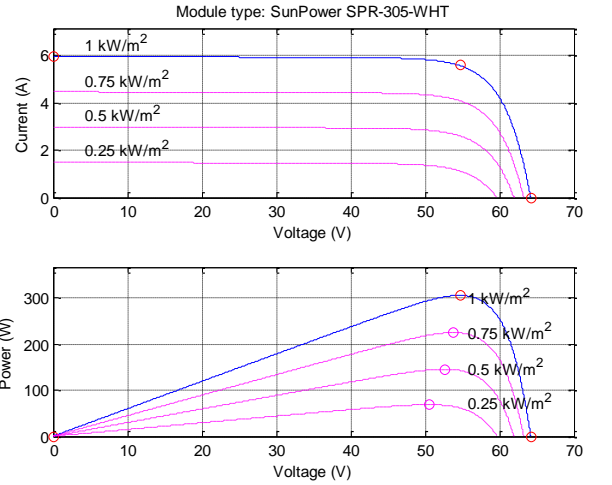


Fig. 5. I-V and P-V characteristics of SunPower SPR 305WHT module with varying irradiance

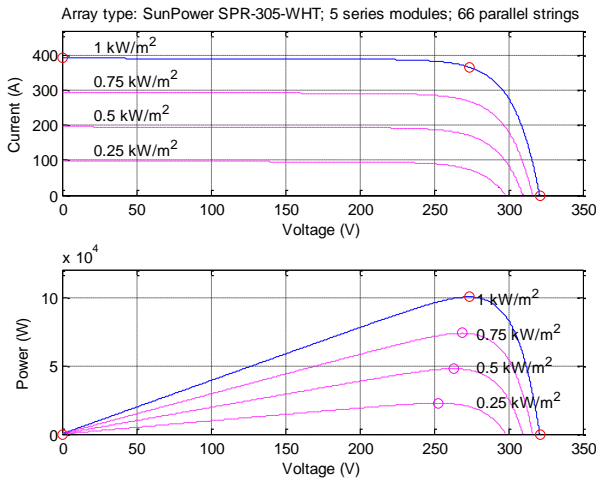


Fig. 6. I-V and P-V characteristics of SunPower 305 WHT array with varying irradiance

PV current changes with the solar irradiation level, and the PV output voltage changes with the temperature of the PV module, which is shown in the following simulation results. Fig. 7 illustrates the P-V characteristics of PV cell with varying temperature and Fig. 8 shows the I-V characteristics of PV cell with variable temperature.

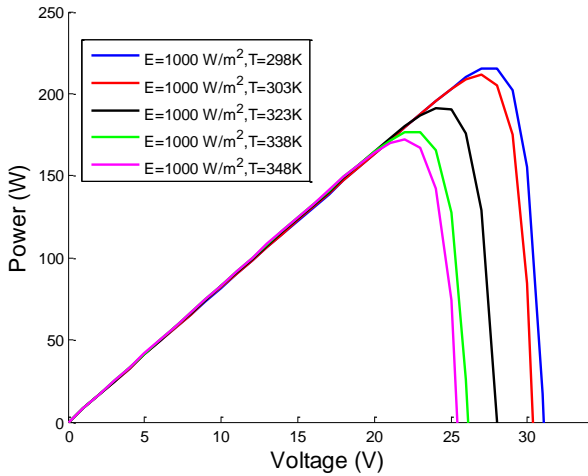


Fig. 7. P-V characteristics of PV cell with varying temperature

For simulation the following parameters are considered. In boost converter the parameters are  $C_{in} = 100\mu\text{F}$ ,  $L = 5 \text{ mH}$ ,  $C_o = 24000\mu\text{F}$  and the DC-link voltage is 500 V DC. The switching frequency for the boost converter is 50 kHz. For classical perturb and observe MPPT, the initial value of  $D$  is 0.5. The upper limit and lower limit of  $D$  is 0.52 and 0.42 respectively. The increment factor of  $D$  is  $3e-4$ . The PV voltage and PV current with respect to change in irradiance is shown in Fig. 10 and Fig. 11 respectively. At normal condition, the PV voltage is around 300V DC and PV current is around 300A for a 100 kW PV installation. The

output DC-link voltage of DC-DC boost converter is kept at 500V DC which is illustrated in Fig. 12.

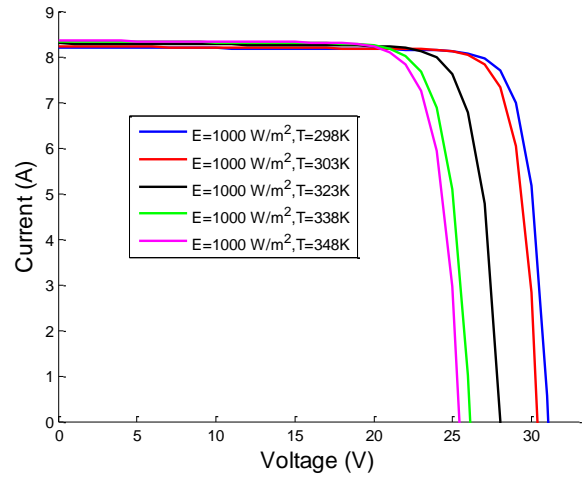


Fig. 8. I-V characteristics of PV cell with varying temperature

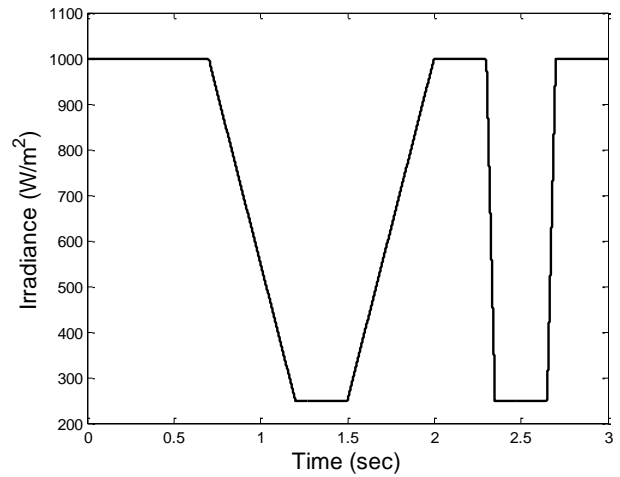


Fig. 9. Change of solar irradiance (simulated)

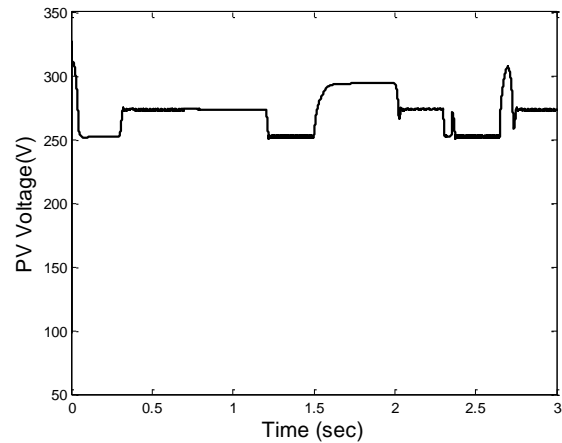


Fig. 10. Change of PV voltage due to change in irradiance

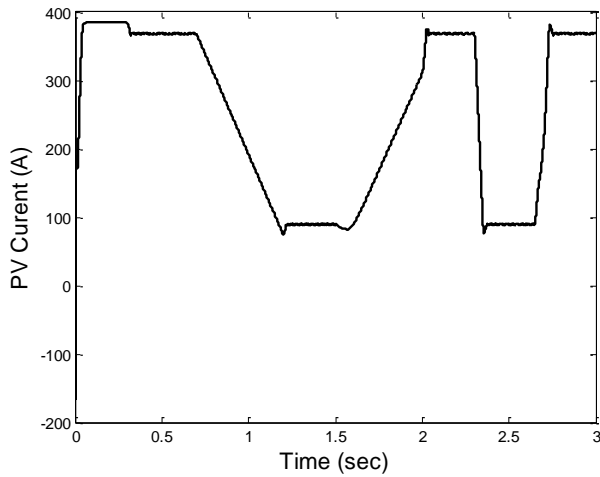


Fig. 11. Change of PV current due to change in irradiance

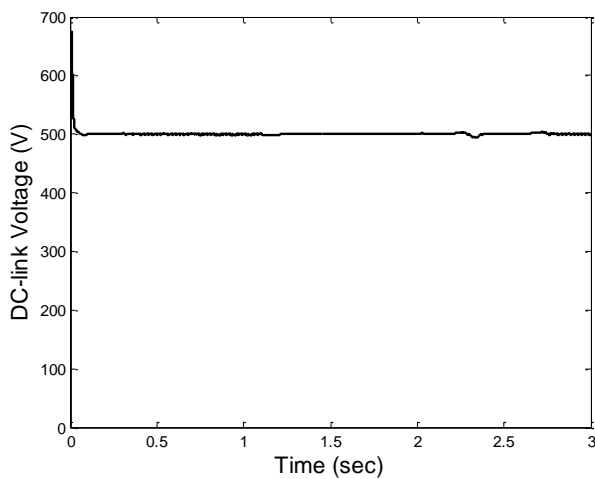


Fig. 12. DC-link voltage (output voltage of boost converter)

## VI. CONCLUSION

This paper provides a detailed design analysis of MPPT technique for stand-alone PV system. Therefore, the first step of designing of such a system is to develop accurate model of PV module and PV array used for the design. This paper considers Sun Power SPR 305 WHT PV module and array. Simulation studies are carried out to understand the output characteristics of the module and array with respect to unpredictable change in solar irradiance and ambient temperature. Classical perturb and observe MPPT is used to track the maximum power. The PCU of PV system comprises

of a DC-DC converter which is used to regulate the output voltage of the system.

## REFERENCES

- [1] A. T. Elsayed, A. A. Mohamed, and O. A. Mohammed, "Dc microgrids and distribution systems: An overview," *Electric Power Systems Research*, vol. 119, pp. 407–417, 2015.
- [2] A. Mohamed, V. Salehi, and O. Mohammed, "Real-time energy management algorithm for mitigation of pulse loads in hybrid microgrids," *IEEE Trans. Smart Grid*, vol. 3, no. 4, pp. 1911–1922, 2012.
- [3] L. Khemissi, B. Khiari, R. Andoulsi, and A. Cherif, "Low cost and high efficiency of single phase photovoltaic system based on microcontroller," *Solar energy*, vol. 86, no. 5, pp. 1129–1141, 2012.
- [4] E. Koutroulis, K. Kalaitzakis, and N. C. Voulgaris, "Development of a microcontroller-based, photovoltaic maximum power point tracking control system," *IEEE Trans. Power Electron.*, vol. 16, no. 1, pp. 46–54, 2001.
- [5] M. G. Villalva, J. R. Gazoli *et al.*, "Comprehensive approach to modeling and simulation of photovoltaic arrays," *IEEE Trans. Power Electron.*, vol. 24, no. 5, pp. 1198–1208, 2009.
- [6] S. A. Rahman, R. Varma, and T. Vanderheide, "Generalised model of a photovoltaic panel," *IET Renewable Power Generation*, vol. 8, no. 3, pp. 217–229, 2014.
- [7] G. Bhuvaneshwari and R. Annamalai, "Development of a solar cell model in matlab for pv based generation system," in *Proc. IEEE India Conference (INDICON)*, 2011, pp. 1–5.
- [8] B. Subudhi and R. Pradhan, "A comparative study on maximum power point tracking techniques for photovoltaic power systems," *IEEE Trans. Sustain. Energy*, vol. 4, no. 1, pp. 89–98, 2013.
- [9] P.-C. Chen, P.-Y. Chen, Y.-H. Liu, J.-H. Chen, and Y.-F. Luo, "A comparative study on maximum power point tracking techniques for photovoltaic generation systems operating under fast changing environments," *Solar Energy*, vol. 119, pp. 261–276, 2015.
- [10] M. Berrera, A. Dolara, R. Faranda, and S. Leva, "Experimental test of seven widely-adopted mppt algorithms," in *Proc. IEEE PowerTech*, 2009, pp. 1–8.
- [11] V. Salas, E. Olias, A. Barrado, and A. Lazaro, "Review of the maximum power point tracking algorithms for stand-alone photovoltaic systems," *Solar energy materials and solar cells*, vol. 90, no. 11, pp. 1555–1578, 2006.
- [12] T. Esmar, P. L. Chapman *et al.*, "Comparison of photovoltaic array maximum power point tracking techniques," *IEEE Trans. Energy Convers.*, vol. 22, no. 2, p. 439, 2007.
- [13] A. Anurag, S. Bal, S. Sourav, and M. Nanda, "A review of maximum power-point tracking techniques for photovoltaic systems," *International Journal of Sustainable Energy*, pp. 1–24, 2014.
- [14] S. Bal and B. C. Babu, "Comparative study between p&o and current compensation method for mppt of pv energy system," in *Proc. Students Conference on Engineering and Systems*, 2012, pp. 1–6.
- [15] M. Killi and S. Samanta, "Modified perturb and observe mppt algorithm for drift avoidance in photovoltaic systems," *IEEE Trans. Ind. Electron.*, vol. 62, no. 9, pp. 5549–5559, 2015.